INSTITUTE REPORT NO. 472

Alterations in Morphology and ERG Spectral Sensitivity After Near IR (1064 nm) Multiple Parafoveal Q-switched Laser Exposure

H. Zwick, S.B. Reynolds,
D.J. Lund, S.T. Schuschereba,
B.E. Stuck, M. Belkin,
and S.A. Silverman

Division of Ocular Hazards Research

September 1992

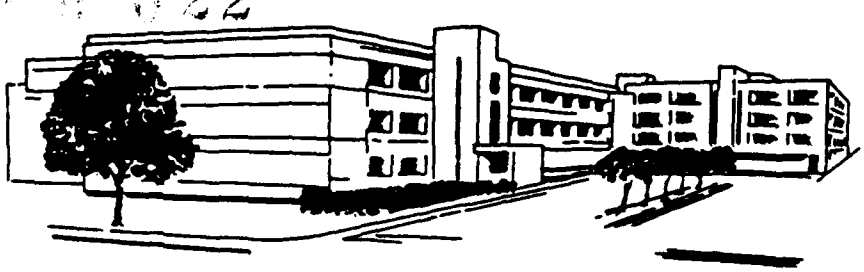

LETTERMAN ARMY INSTITUTE OF RESEARCH PRESIDIO OF SAN FRANCISCO CALIFORNIA 94129

Alterations in morphology and ERG spectral sensitivity after near IR (1064 nm) multiple parafoveal Q-switched laser exposure, H. Zwick, et al.

This document has been approved for public release and sale; its distribution is unlimited.

Destroy this report when it is no longer needed. Do not return to the originator.

Citation of trade names in this report does not constitute an official endorsement or approval of the use of such items.

The experimental studies of the author described in this report were reviewed and approved by the Institutional Review Committee/Animal Care and Use Committee at Letterman Army Institute of Research. The manuscript was peer reviewed for compliance prior to submission for publication. In conducting the research described here, the author adhered to the "Guide for the Care and Use of Laboratory Animals," DHEW Publication (NIH) 86-23.

This material has been reviewed by Letterman Army Institute of Research and there is no objection to its presentation and/or publication. The opinions or assertions contained herein are the private views of the author(s) and are not to be construed as official or as reflecting the views of the Department of the Army or the Department of Defense. *(AR 360-5)*

14SEP92

GEORGE J. BROWN
COL, MC
Commanding

(date)

REPORT DOCUMENTATION PAGE

Form Approved
OMB No. 0704-0188

1a. REPORT SECURITY CLASSIFICATION Unclassified	1b RESTRICTIVE MARKINGS
2a. SECURITY CLASSIFICATION AUTHORITY	3. DISTRIBUTION/AVAILABILITY OF REPORT Approved for public release; Distribution is UNLIMITED.
2b. DECLASSIFICATION/DOWNGRADING SCHEDULE	
4. PERFORMING ORGANIZATION REPORT NUMBER(S) Institute Report # 472	5. MONITORING ORGANIZATION REPORT NUMBER(S)
6a. NAME OF PERFORMING ORGANIZATION Division of Ocular Hazards 6b. OFFICE SYMBOL (If applicable) SGRD-ULZ-OH	7a. NAME OF MONITORING ORGANIZATION US Army Medical Research and Development Command
6c. ADDRESS (City, State, and ZIP Code) Letterman Army Institute of Research Bldg 1110 Presidio of San Francisco, CA 94129-6800	7b. ADDRESS (City, State, and ZIP Code) Ft. Detrick Frederick, MD 21701-5012
8a. NAME OF FUNDING/SPONSORING ORGANIZATION 8b. OFFICE SYMBOL (If applicable)	9. PROCUREMENT INSTRUMENT IDENTIFICATION NUMBER
8c. ADDRESS (City, State, and ZIP Code)	10. SOURCE OF FUNDING NUMBERS PROGRAM ELEMENT NO. 3002 / PROJECT NO. D819 / TASK NO. AA / WORK UNIT ACCESSION NO. 245

11. TITLE (Include Security Classification)
(U) Alterations in morphology and ERG spectral sensitivity after near IR (1064 nm) multiple parafoveal Q-switched laser exposure

12. PERSONAL AUTHOR(S) H. Zwick, S.B. Reynolds, D.J. Lund, S.T. Schuschereba, B.E. Stuck, M. Belkin, and U.S. Silverman

13a. TYPE OF REPORT	13b. TIME COVERED	14. DATE OF REPORT (Year, Month, Day)	15. PAGE COUNT
Final	FROM _____ TO _____	1992, Sep 1	22

16. SUPPLEMENTARY NOTATION

17. COSATI CODES			18. SUBJECT TERMS (Continue on reverse if necessary and identify by block number)
FIELD	GROUP	SUB-GROUP	spectral sensitivity, fovea, retinal fibrosis, reparative functions, photoreceptors

19. ABSTRACT (Continue on reverse if necessary and identify by block number)

In this investigation, we examined the effect of near-infrared intense macular laser exposure on the non-human primate focal ERG spectral sensitivity function. Five cynomologous monkeys were exposed to two parafoveal Q-switched Neodymium (1064 nm) laser pulses at approximately 4 millijoules Total Interocular Energy (TIE). Exposures varied in degree of overlap through the superior portion of the fovea. Focal ERG spectral sensitivity was measured in the foveal region using a synchronous detection technique. Alteration in the long wavelength region of the focal ERG spectral sensitivity function was observed in all animals. This alteration could indicate a dominant presence of the long wavelength primate cone system. The dominance may be the result of neural disinhibitory effects of damaged photoreceptors and the complications of retinal fibrosis on normal receptor activity and orientation as well as normal retinal receptor reparative functions.

20 DISTRIBUTION/AVAILABILITY OF ABSTRACT ☒ UNCLASSIFIED/UNLIMITED ☐ SAME AS RPT ☐ DTIC USERS	21. ABSTRACT SECURITY CLASSIFICATION Unclassified
22a. NAME OF RESPONSIBLE INDIVIDUAL GEORGE J. BROWN, COL, MC, Commanding	22b. TELEPHONE (Include Area Code) (415) 561-3600 22c. OFFICE SYMBOL SGRD-ULZ

DD Form 1473, JUN 86 *Previous editions are obsolete.*

Abstract

In this investigation, we examined the effect of near-infrared intense macular laser exposure on the non-human primate focal ERG spectral sensitivity function. Five cynomologous monkeys were exposed to two parafoveal Q-switched Neodymium (1064 nm) laser pulses at approximately 4 millijoules Total Interocular Energy (TIE). Exposures varied in degree of overlap through the superior portion of the fovea. Focal ERG spectral sensitivity was measured in the foveal region using a synchronous detection technique. Alteration in the long wavelength region of the focal ERG spectral sensitivity function was observed in all animals. This alteration could indicate a dominant presence of the long wavelength primate cone system. The dominance may be the result of neural disinhibitory effects of damaged photoreceptors and the complications of retinal fibrosis on normal receptor activity and orientation as well as normal retinal receptor reparative functions.

Alterations in morphology and ERG spectral sensitivity after near IR (1064 nm) multiple parafoveal Q-switched laser exposure -- H. Zwick, S.B. Reynolds, D.J. Lund, S.T. Schuschereba, B.E. Stuck, M. Belkin, and M.S. Silverman

Introduction

Photic damage from intense light exposure initiates a complex reorganization of retinal processing and possible restoration of visual function (1,2). If a group of photoreceptors are damaged within or peripheral to the fovea, output will be diminished. Decreased output will reduce the neural lateral inhibition that such receptors normally exert on adjacent receptor systems. Harwerth and Sperling (3) showed that intense repetitive exposure to 520 nm light decreased the mid-wavelength cone input to the increment spectral sensitivity function of the rhesus monkey, resulting in a spectral sensitivity function satisfactorily fitted by the long wavelength and short wavelength cone systems. Zwick and Beatrice (4) showed a similar but more permanent effect using coherent 514 nm light. These effects were not weak effects, as they lasted longer than a year and progressed in the absence of continued stimulation (5).

Although the initial investigations of such effects lay in the photic non-thermal damage mechanism domain, recent investigations indicate that thermal and mechanical mechanisms of retinal damage may induce similar effects on visual function via replacement mechanisms of damaged or missing photoreceptors. Punctate damage from minimal spot foveal laser exposure alters the slope of the rhesus contrast sensitivity function, making it slightly more sensitive at lower spatial frequencies (2). This alteration in slope may result from reduction in foveal receptor control of parafoveal receptor output as well as passive receptor movement of adjacent normal receptor systems. Such movement processes can allow restoration of the foveal receptor matrix (5), critical in maintaining foveal acuity. However, such passive movement receptor processes may indeed modulate neural lateral influence by changing the spatial relationships among foveal and parafoveal receptors.

The above investigations involved changes induced on foveal receptor mechanisms by partial removal of foveal receptor systems. Recent human laser accident cases have involved parafoveal damage with significant effects on foveal function (6). In one case, parafoveal

laser injury produced a central scotoma that lasted several weeks before resolving to a smaller paracentral scotoma consistent with the parafoveal retinal site of injury. In a second case, severe retinal scarring followed multiple parafoveal injury and produced a central absolute arcuate scotoma that decreased in size by about half during the first month post-exposure and showed no subsequent change. In this latter case, no recovery in acuity or contrast sensitivity loss was observed during a sixteen-month period, as opposed to the former case in which scarring was minimal and acuity returned to near-normal levels following a 3 to 5 month observation period.

In the present investigation, we assessed the role of acute laser exposure to induce macular retinal fibrosis and alteration in neural retinal activity and determined how such retinal change is relayed through the visual nervous system (7). Our assessment employs electroretinography, retinal histology, and measurement of brain enzyme change associated with laser-induced retinal scar pathology.

Methods

Five cynomologous monkeys were used in this experiment. Laser exposure consisted of two Neodymium (1064 nm) Q-switched (20 nanoseconds) pulses delivered successively within several seconds of each other on either side of the fovea with variation in exposure overlap. The laser beam produced a minimal retinal spot size of 50 microns. All laser exposures were done under funduscopic control in anesthetized animals. Pulses ranged from 3 to 6 millijoules TIE (Total Interocular Energy) and produced immediate vitreal hemorrhage (bleeding into the vitreous from the exposure site; such bleeding resolved in 24 to 48 hours and was a significant factor in production of retinal fibrosis). Foveal overlap of these parafoveal exposures ranged from about 5 to 50 percent of the fovea. Ophthalmoscopy and retinal photography were made at various intervals after exposure through 15 months post-exposure.

Foveal ERG spectral sensitivity was measured using a synchronous detection technique (8,9). A fundus camera was employed to view the retina and to direct the test beam onto the fovea. ERG measurements were always made in the same foveal region pre- and post- exposure. An automated goniometer was used to position the test spot on the anesthetized animal's macula. The test spot was 3 degrees. (To minimize scatter from complex retinal scar formation and to minimize additional adaptive effects on the expression of macula retinal reparative processes, a background channel was not employed.) Test

light intensity was varied by two opposing circular optical density wedges with a dynamic range of about four log units. Interference filters from 400 to 700 nm with half-band width maxima of 10 nm were used to vary wavelength. An equal energy spectrum was produced by bringing energy output at all filters to the same level as that produced at the 600 nm filter. The test light was continuously flickered by placing a 50% duty cycle variable rate light chopper at a focal point in the test beam light channel. A Stanford Research Systems dual phase lock-in amplifier was used to process the repetitive ERG via a Burian Allen bipolar contact lens electrode with input referenced to the test light frequency.

A servo loop maintained a constant voltage criterion of 0.5 uv rms by controlling the direction of a wedge motor; i.e., when the repetitive ERG signal dropped below the criterion voltage, the wedge density decreased; when the signal exceeded this criterion voltage, wedge density increased. In this manner, threshold voltage levels were obtained across the visible spectrum. Approximately 2 minutes of stable data were measured at each wavelength. Variability during this time never exceeded +/- 0.2 log units. The reciprocal of these measurements are plotted as log relative sensitivity for various wavelength points. Spectral sensitivity measurements were made at each wavelength and normalized for an equal energy spectrum. At least two successive baseline spectral sensitivity measurements within the above variability range were required prior to laser exposure.

Retinal and brain histopathology were performed on one animal (Cyno38) in which corresponding pre- and post-exposure ERG spectral sensitivity measures were obtained. Thin section light microscopy of the retina (10) was performed on one animal (Cyno38). In these animals, cortical brain tissue was sectioned and examined for cytochrome oxidase activity (11,12).

Results

Figures 1 and 2 show post-exposure retinal scar formation produced by parafoveal vitreal hemorrhagic exposures for two animals. These two animals represent extremes of parafoveal lesion overlap onto the fovea. In cyno24, (Figure 1) the retinal scar is more compact with more significant scar formation between exposure sites. Evidence of retinal scar tissue extending outside the lesion seemed more noticeable in animals having a greater degree of lesion overlap. In cyno36, (Figure 2) parafoveal exposure sites minimally overlapped. Bridging scar tissue

between these parafoveal sites formed adjacent to and above the foveal region within the first week post-exposure.

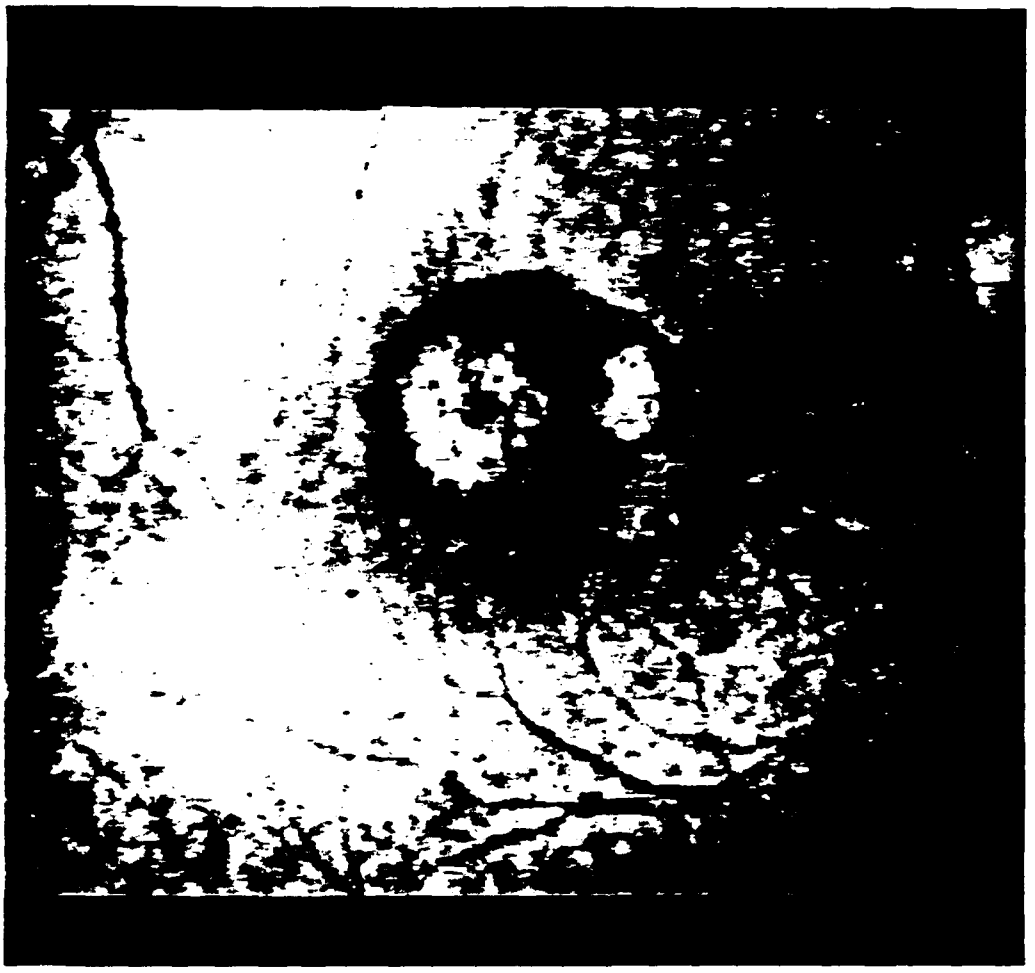

Figure 1. Post exposure fundus photograph of cyno24 showing example of parafoveal lesion overlap. In this animal exposures overlapped about 50 percent of the fovea.

Figure 2. Post exposure fundus photograph of cyno36 showing example of minimal parafoveal lesion overlap. The bridging of the two lesions in this animal is apparent. Exposure overlap was minimal; i.e., about 5 percent.

Figure 3 shows the effect of varying the flicker frequency on the ERG spectral sensitivity function obtained with a 0.5 uv rms criterion response. The 12 Hz curve shows a greater overall sensitivity relative to the 25 and 40 Hz functions. This function is at least a log unit greater in sensitivity than either the 25 or 40 Hz functions and peaks between 500 and 520 nm. The 25 Hz spectral sensitivity function typically peaks at 600 nm or has a broader shoulder in the longer wavelength region (>580 nm) relative to the 40 Hz function; also, it is about 0.2 of a log unit more sensitive across the visible spectrum than the 40 Hz function. The longer wavelength peak of the 25 Hz (600 nm) versus that of the 40 Hz spectral sensitivity function (560 nm) may reflect stronger interactions between parafoveal and long wavelength cone receptor processes than are present at the more photopic 40 Hz function. These spectral sensitivity characteristics were measurable at least 3 degrees eccentric to the fovea with corresponding decreases in 40 Hz spectral sensitivity in contrast to slight increases in sensitivity at 12 Hz. (Although we do not have systematic data on sensitivity changes, local ERG spectral sensitivity changes could be obtained under these recording conditions.)

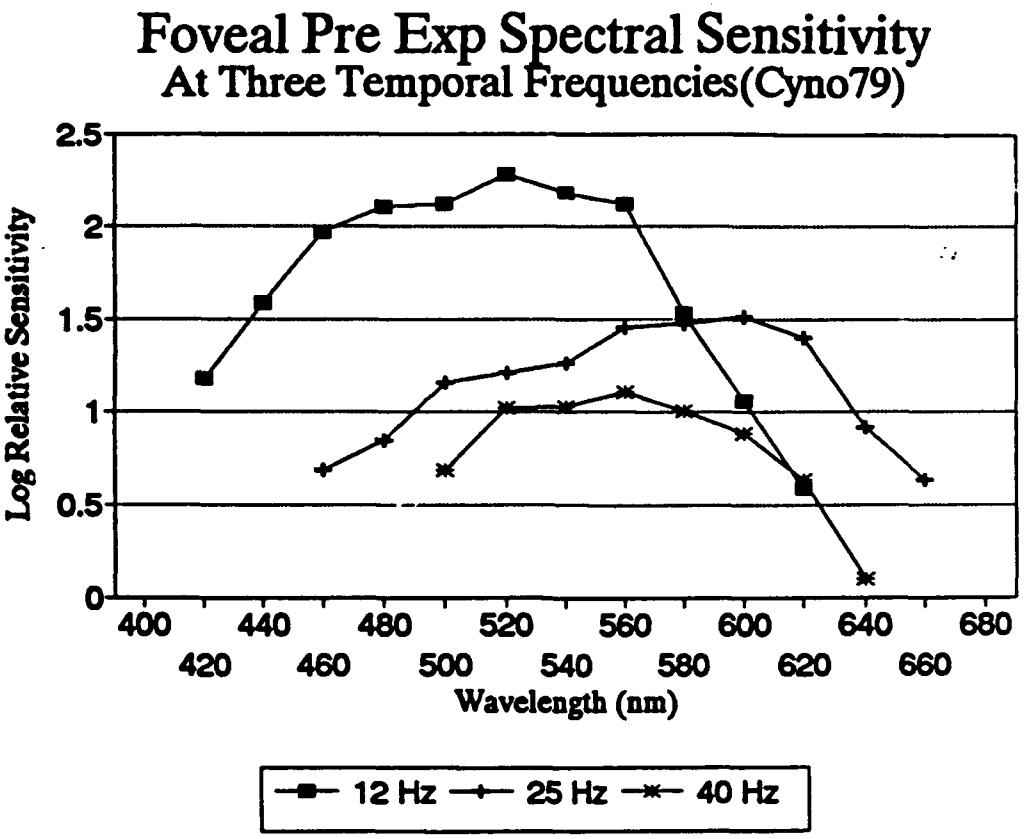

Figure 3. ERG focal spectral sensitivity functions measured at the fovea for three flicker frequencies at 12, 25, and 40 Hz is shown for one non-irradiated animal. Spectral sensitivity measured at 12 Hz shows maximum overall sensitivity and a peak at about 500 to 520 nm. At 25 Hz, maximum focal spectral sensitivity is about 580 nm; at 40 Hz, maximum spectral sensitivity shifts to 560 nm.

Figures 4 through 10 present the pre- and post-exposure effects of parafoveal laser exposure for each of five irradiated animals. In Figure 4A, recovery for Cyno17 is shown from the initial hours of post-exposure through 1 year post-exposure. The initial loss as compared to the unexposed eye is maximum beyond 600 nm with a peak shift in maximum sensitivity toward the mid-wavelength cone region. In Figure 4B, the Smith and Porkorny (13) long wavelength cone fundamental (L Cone) was fitted to the post-exposure maxima of the 2 hour and 15 day functions. The long wavelength fundamental makes a good fit with these post-exposure functions because of the decrease in spectral sensitivity beyond 560 nm.

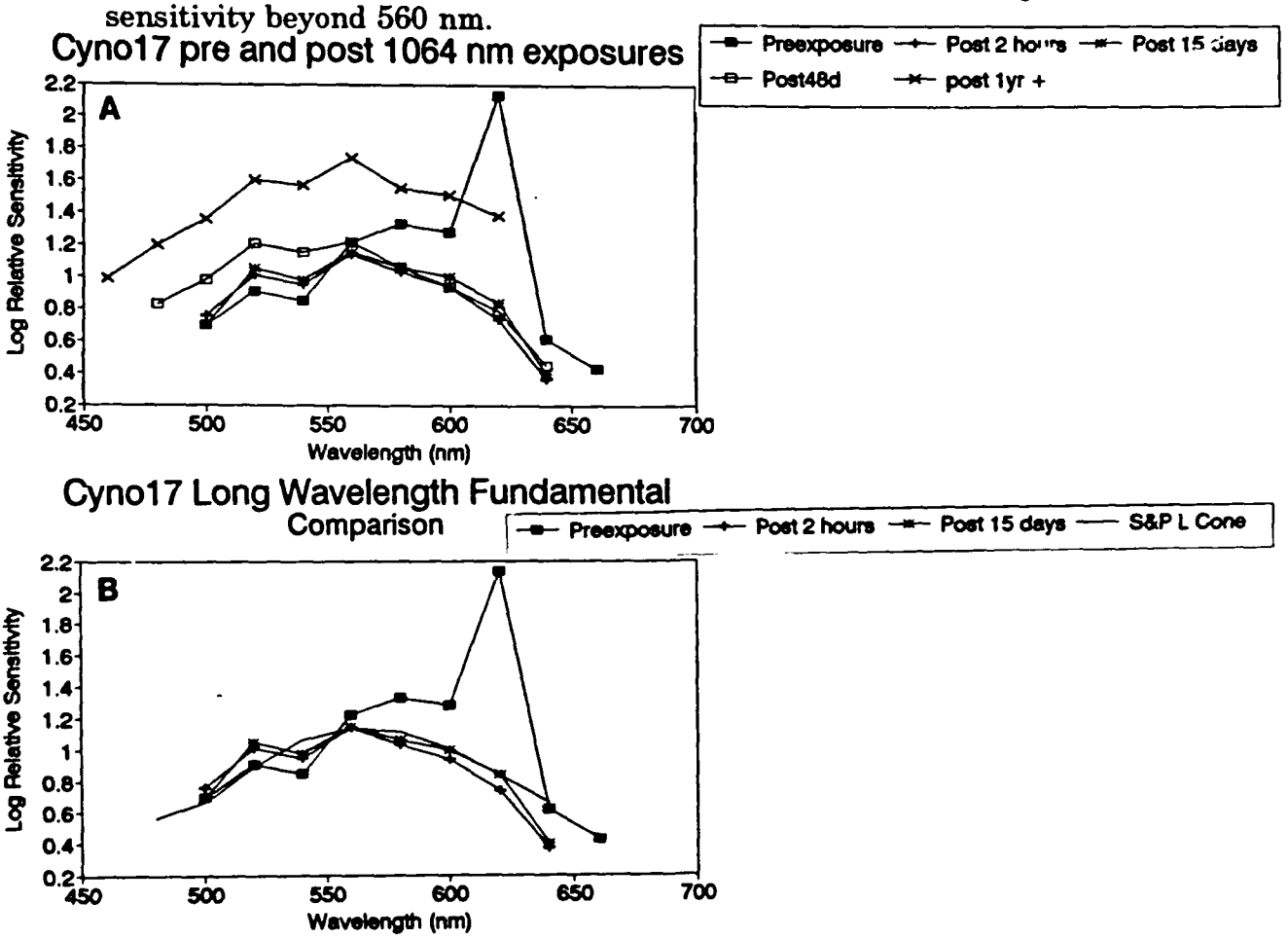

Figure 4. Figure 4A shows recovery for Cyno17 from ERG spectral sensitivity measurements made 2 hours post-exposure to comparable measurements made more than 1 year post-exposure. Figure 4B shows the fit of the Smith and Pokorny long wavelength cone fundamental normalized at 560 nm with the 2 hour and 15 day post-exposure ERG spectral sensitivity functions.

A similar trend is apparent in Figure 5 for Cyno24. Maximum post-exposure sensitivity loss occurs in the long wavelength region with a maximum spectral sensitivity from 560 to 660 nm (Figure 5A). The long wavelength fundamental (Figure 5B) makes a good fit with the post-exposure data at 9 and 21 days, although this fit is weaker below than above 560 nm.

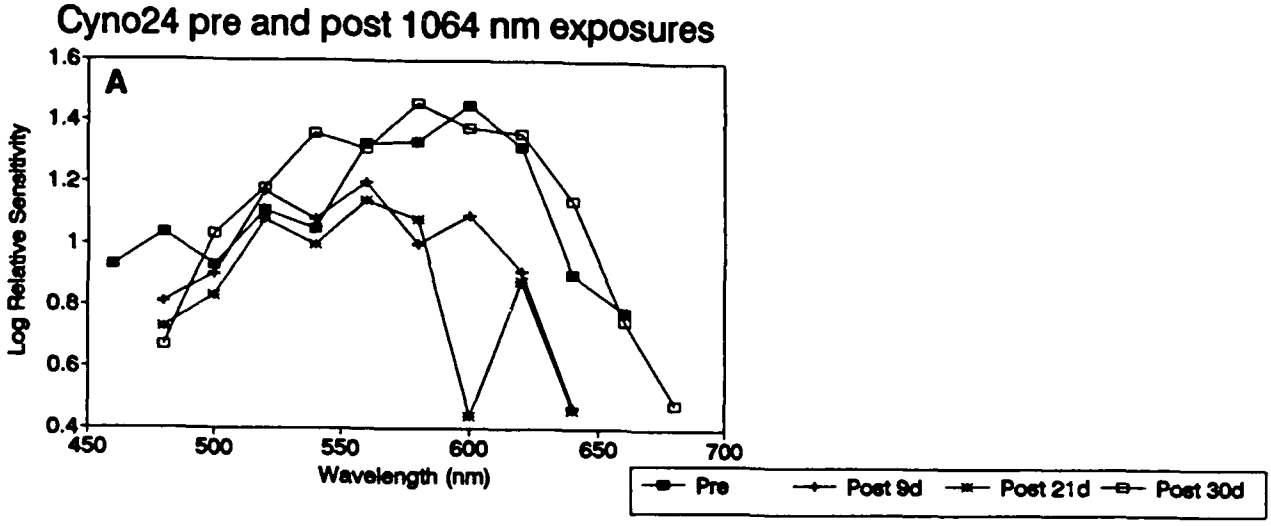

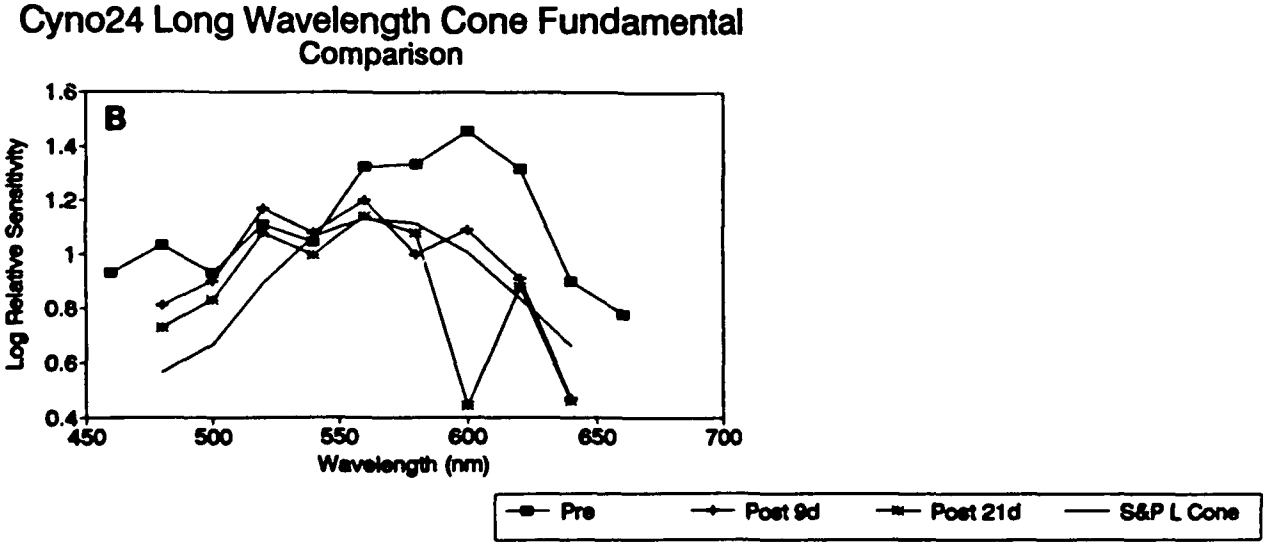

Figure 5. Figure 5A shows recovery for Cyno24 from 9 days to 30 days post-exposure. Figure 5B shows the fit of the Smith and Pokorny Long wavelength cone fundamental normalized at 560 nm with post-exposure ERG spectral sensitivity measurements made at 9 and 30 days post-exposure. The fit of these functions is better above than below 560 nm.

In Cyno33 (Figure 6A), exposure resulted in shifting the peak spectral sensitivity from 580 to 520 nm with a secondary peak or plateau through 540 to 560 nm. The long wavelength fundamental fits best beyond 560 nm (Figure 6B) with a weaker fit below 560 nm, similar to Cyno24.

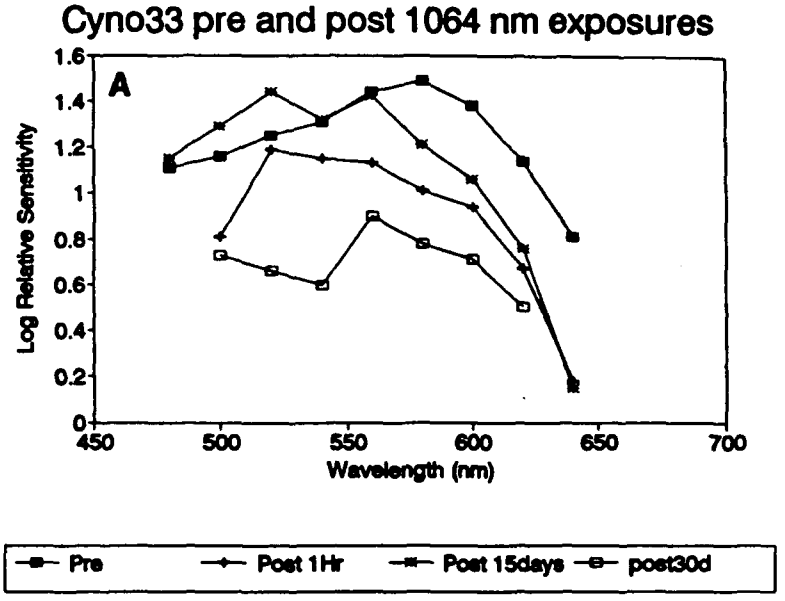

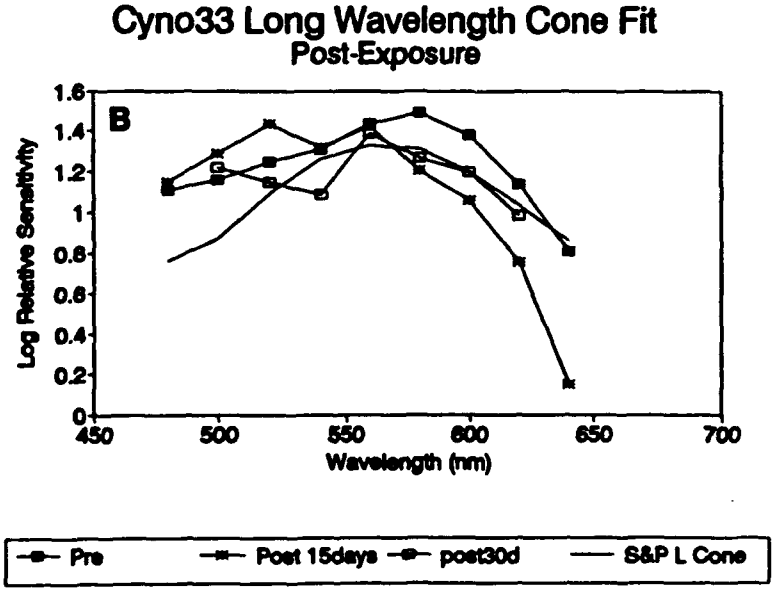

Figure 6. Figure 6A shows recovery for Cyno33 from 1 hour to 30 days post-exposure. Figure 6B shows the fit of the Smith and Pokorny long wavelength cone fundamental normalized at 560 nm with the post 1 hour and 30 day functions. This fit is also better above than below 560 nm.

In Cyno36 (Figure 7) measurements of spectral sensitivity showed the smallest absolute loss in sensitivity but a definite shift in peak spectral sensitivity from 580 to 560 nm. The post-exposure function is best fitted above 560 nm with the long wavelength fundamental and below 560 nm by the mid-wavelength cone fundamental of Smith and Pokorny (13).

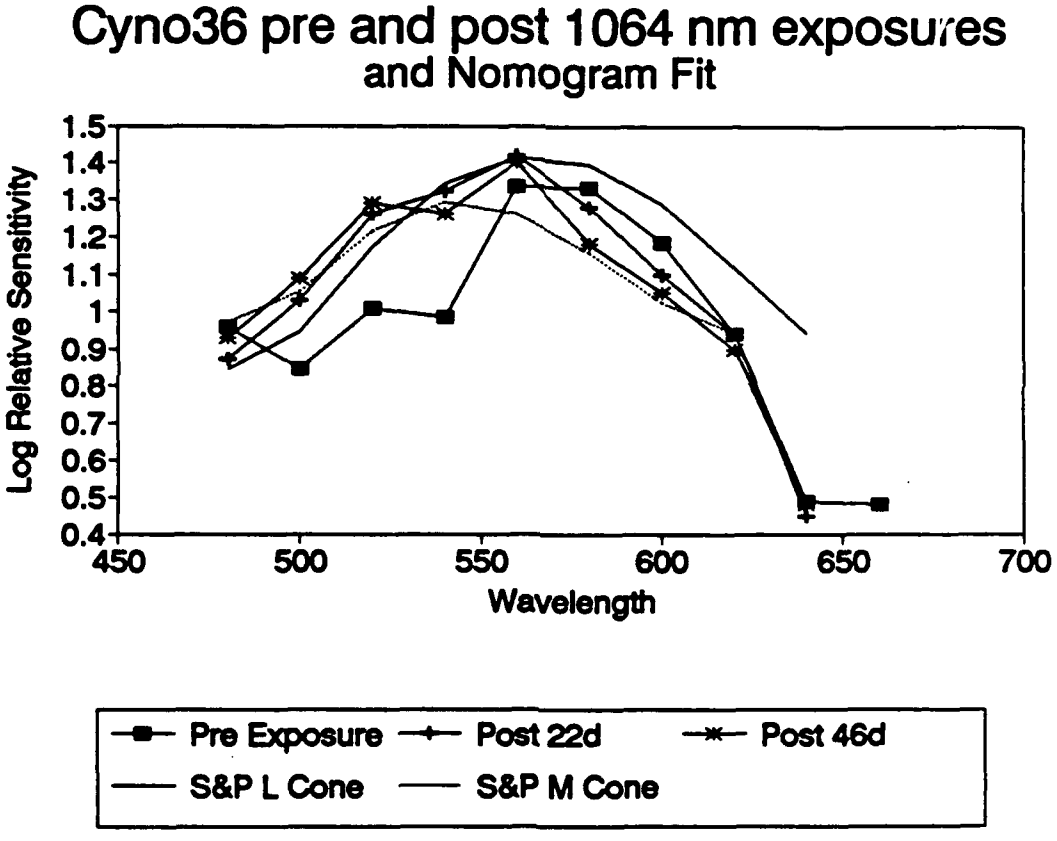

Figure 7. Figure 7 shows recovery for Cyno36 at 22 and 46 days post-exposure. The long wavelength cone fundamental is normalized with both post-exposure functions at 560 nm and the mid-wavelength cone fundamental is normalized with both functions at 540 nm.

The ERG spectral sensitivity measured at the fovea and at the edge of the scar for Cyno24 is presented in Figure 8. Although recovery exceeds pre-exposure levels for the fovea, it is considerably reduced for the parafoveal measurement at the edge of the scar. Although foveal and scar spectral sensitivity measurements were possible at 25 Hz, no spectral sensitivity measurements were possible at 12 Hz, either in the fovea or on the edge of the scar. The inability to make such measurements suggests severe reduction in rod and other parafoveal receptor activity throughout the macular region.

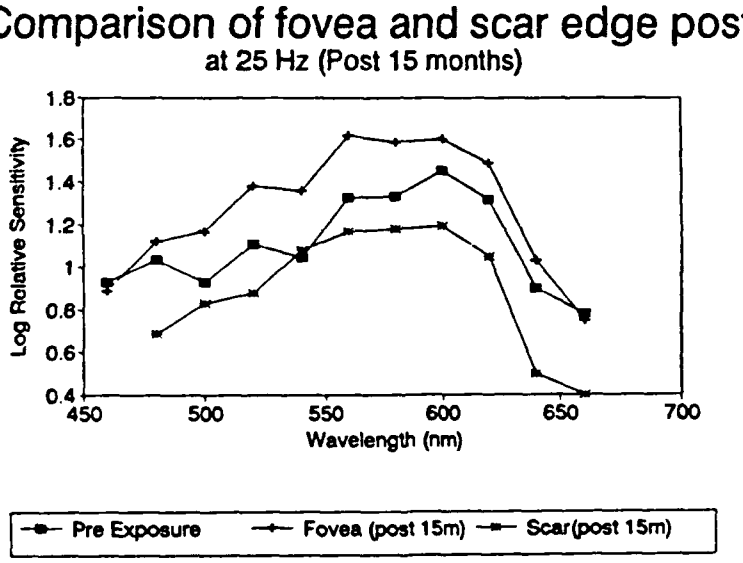

Figure 8. Figure 8 shows the ERG spectral sensitivity measured at the fovea and at the edge of the scar for Cyno24 measured at 25 Hz flicker frequency.

Spectral sensitivity function measurements in Cyno38 show greater deficits at 5 weeks post-exposure for 40 versus 25 Hz (Figure 9A). On the other hand, the fit of the long wavelength cone fundamental for both the 25 and 40 Hz post-exposure functions is slightly better than that for the pre-exposure normalized functions (Figure 9b).

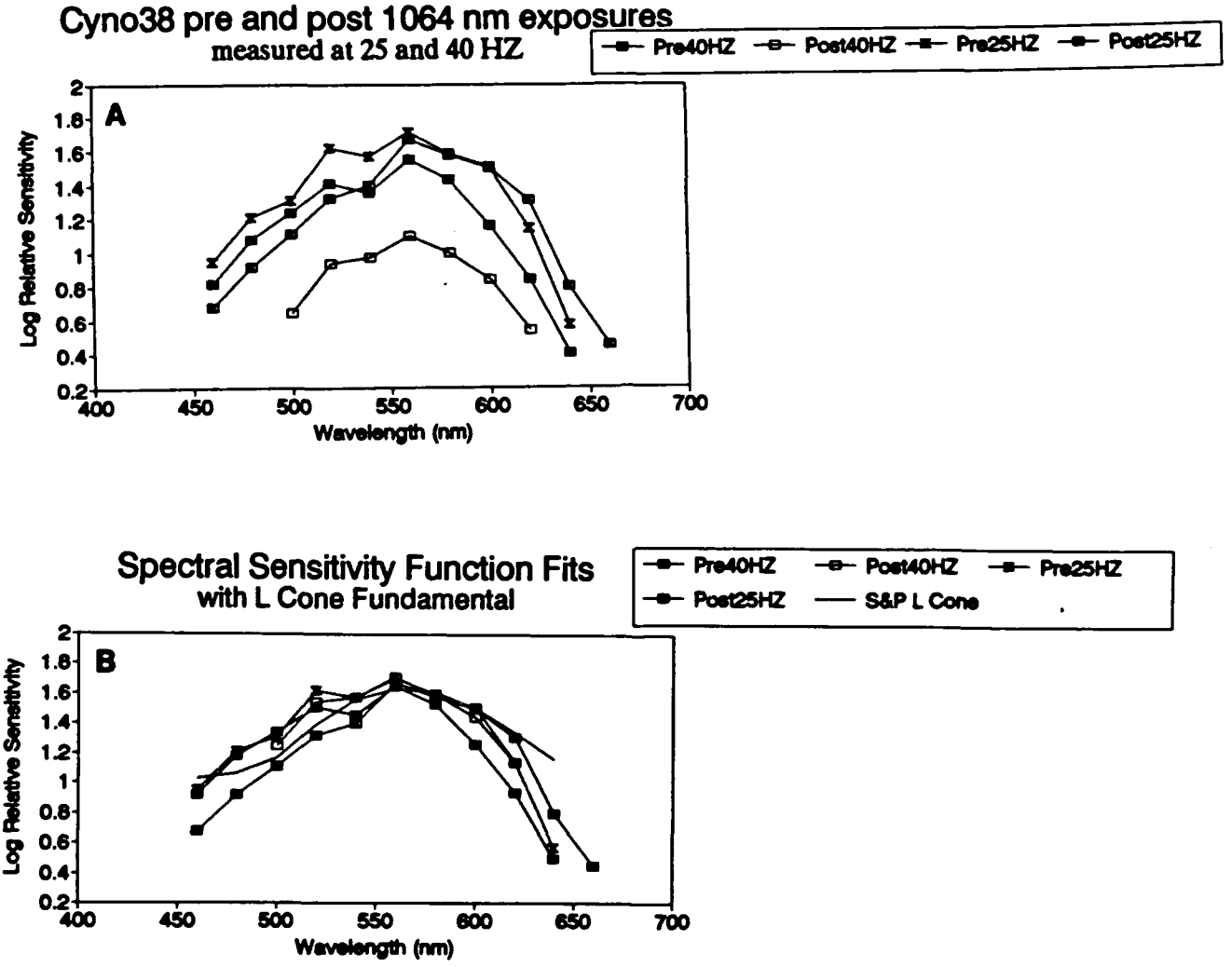

Figure 9. Figure 9A shows the post-exposure ERG spectral sensitivity functions at 25 and 40 Hz for Cyno38. Depression at 40 Hz at 5 weeks post-exposure is greater for the 40 vs the 25 Hz function.

Figure 9B shows a good fit with the long wavelength cone fundamental of the post-exposure functions relative to pre-exposure functions.

Light microscopy from this animal (Cyno38) is shown in Figure 10a and 10b. Laser exposures were overlapped the most in this animal. Post-exposure scar formation occurred both within and peripheral to the overlapping macular exposure sites. Figure 10a is a light micrograph of a retinal section through the lesion at about 3 months post-exposure. An arrow designates an area of this section showing scar formation within the retina. Figure 10b is 10x higher magnification showing fibroblast-like cells (F) and glial-like cells (G) present in the retinal scar. The foveal pit has been severely damaged in this retina due to overlapping exposures and a retinal hole that formed very close to the fovea. The production of such holes results from either direct hemorrhagic exposure levels or are formed subsequently by retinal non-elastic collagen fiber traction mechanisms associated with retinal scar. This observation may underlie the greater post-exposure ERG spectral sensitivity deficit observed at 40 Hz as compared with spectral sensitivity measured at 25 Hz.

Photoreceptor survival increases with distance from the foveal region, and is better in the superior to inferior direction than it is from the nasal to temporal direction away from the fovea. Peripheral to the macula, a slight, selective loss of rod photoreceptors may have occurred in this retina.

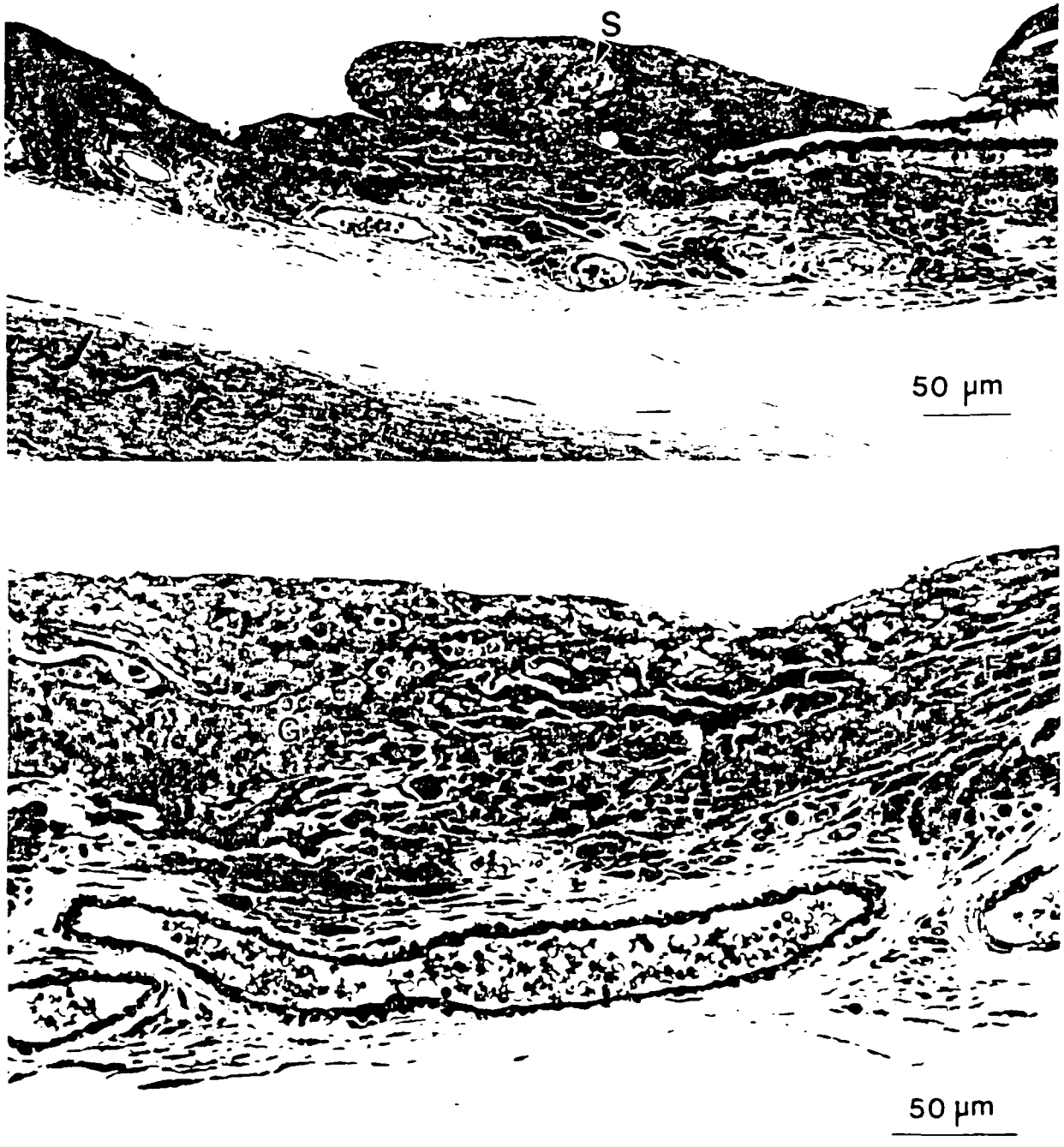

Figure 10a and 10b. Figure 10a is a light micrograph of a retinal section through the lesion (Cyno38). An arrow designates an area of this section showing scar formation within the retina.

Figure 10b is 10x higher magnification showing fibroblast-like cells (F) and glial like cells (G) present in the retinal scar.

Figure 11 shows cytochrome oxidase activity in the right visual cortex (occipital operculum) for Cyno38. Ocular dominance patterns are seen as alternating dark and light strips (small arrowheads) toward the foveal representation (marked by an X) in the primary visual cortex. The presence of ocular dominance bands, seen most clearly in the darkly staining layer 4, presumably reflects unequal activation of eye inputs into the visual cortex. The dark bands represent the non-exposed areas of the follow eye while the lighter bands represent the areas from the exposed eye. These alternating bands extend left from the foveal representation to an area where banding is no longer visible, reflecting normal retinotopic input to this cortical area.

The affected area extends about 5 or 6 degrees (about 15 mm) from the fovea and represents a cortical magnification factor for morphological damage of the retina on the primary visual cortex of about 7.5, assuming suppression of retinal macula input over an area of approximately 2 mm. This factor may vary in other animals in which foveal damage is less severe due to lesser degree of overlapping parafoveal exposure as well as the absence of secondary exposure effects such as foveal retinal hole formation.

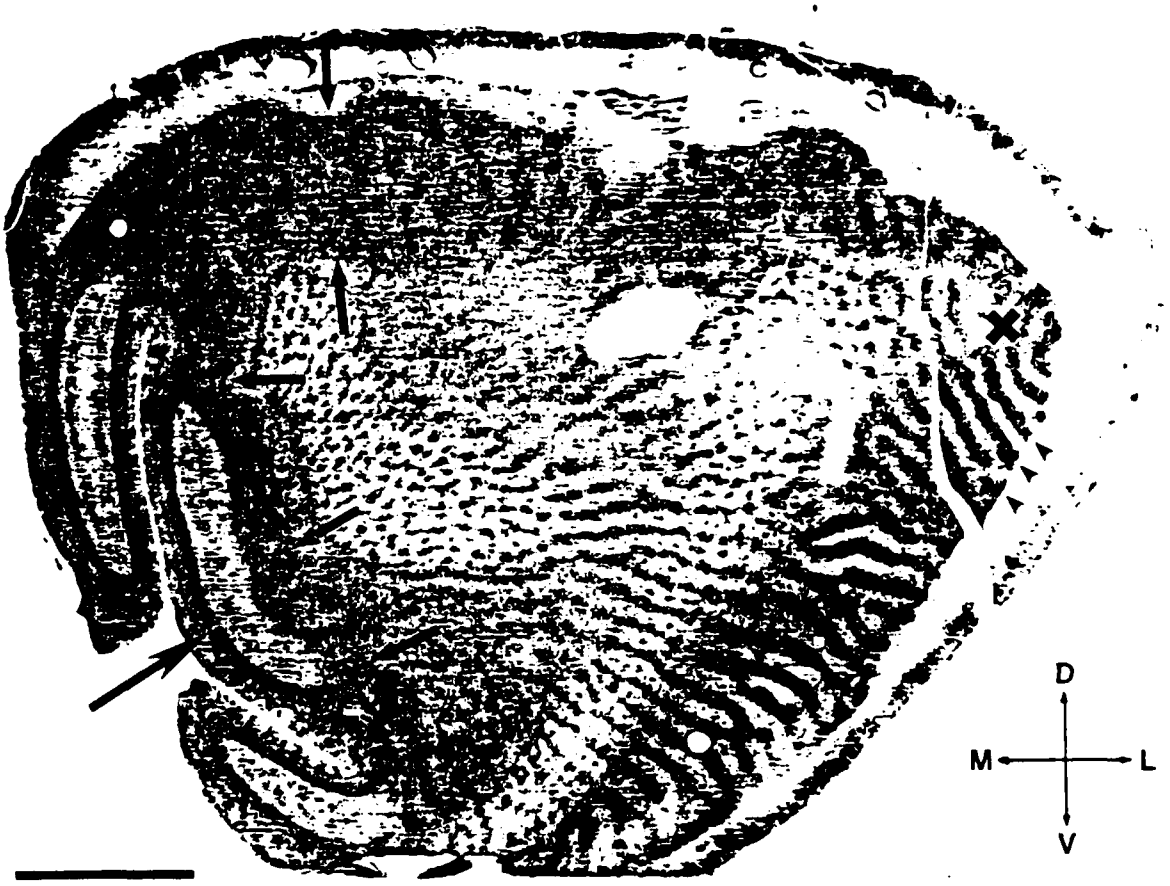

Figure 11. Cytochrome oxidase staining pattern in the right visual cortex (occipital operculum) about 2 months after macular-induced laser damage. The foveal representation is marked by an X. The more peripheral retinotopic representation is represented by a more homogeneous darkly staining area, which represents the normal appearance of layer 4, indicating that both eyes are activating cortex equally about 5 to 6 degrees from the foveal region. Layer 4 viewed perpendicular to the cortical surface at the far edge of the tissue (large arrow) is continuous (has no light and dark discontinuities that indicate ocular dominance columns) further showing that cortical activation from both eyes is normal. Anatomical coordinates: M = medial; D = dorsal; L = lateral; and V = ventral. Scale = 5mm.

Discussion

Parafoveal retinal damage in all animals produced a reduction in ERG spectral sensitivity and shift in most animals in the peak of the 25 Hz spectral sensitivity toward the middle visible wavelengths. Recovery required from several months to more than one year. Complete recovery required more than one year; i.e., complete return to the pre-exposure shape of the ERG spectral sensitivity function. Several explanations of these findings are pertinent to this discussion.

One possible explanation is that stray light onto surrounding parafoveally damaged retinal areas induced retinal rod activity which accounted for the shift toward the shorter wavelengths. However, direct measurements of spectral sensitivity made on the scar or at the edge of the scar resulted in either no measurable activity or significantly diminished activity. The earliest shifts in spectral sensitivity measured at the fovea reflect neither the sensitivity of the rod system nor the shape of the rod spectral sensitivity function (Figure 3). In all post-exposure measurements the best fitting post-exposure function was obtained with the long wavelength cone fundamental alone or in combination with the mid-wavelength cone fundamental. Post-exposure measurements of the 12 Hz spectral sensitivity were significantly diminished in all animals or not measurable at all in at least one animal post-exposure, as compared with robust pre-exposure measurements made at 12 Hz flicker frequency (Figure 3). These data argue that parafoveal rod sensitivity to possible stray light was significantly attenuated, negating its direct contribution to foveal ERG spectral sensitivity measurements.

Alternatively, damage to specific macula receptor systems may have caused the alteration in the shape of the ERG spectral sensitivity function. Both long and mid-wavelength cones are present in the parafoveal areas damaged by laser exposure. Because of variation in parafoveal damage overlap and size of the test spot, both foveal and parafoveal receptor systems were sampled to some degree. Therefore, reduced input from parafoveal receptor systems might play a role in both overall sensitivity which was recorded and in shifts of spectral sensitivity functions. Furthermore, recent studies suggest that direct loss of mid-wavelength cones could have resulted from frequency doubling of 1064 nm laser light, which produced intense 532 nm stimulation, thereby directly damaging the mid-wavelength cone system (14).

The 25 Hz function is usually more sensitive to the longer wavelengths or else fails to match either the photopic spectral or the 40 Hz function. Therefore, the alterations in shape observed in these functions may be more indicative of the removal or attenuation of neural lateral receptor influence of parafoveal receptors rather than the straight-forward reduction in neural input of these receptors to the receptor "pool" underlying the pre-exposure 25 Hz spectral sensitivity function. In previous experiments using the identical focal ERG spectral sensitivity technique, foveal rather than parafoveal damage was induced by acute laser exposure (9). Post-exposure measurements of foveal ERG spectral sensitivity revealed an increase in short wavelength spectral sensitivity with a peak appearing at about 500 nm, suggesting that direct foveal damage may release parafoveal retinal processes. No such intrusion was observed in the present experiment. Furthermore, evidence for an increased long wavelength cone dominance in the 25 Hz ERG spectral sensitivity function was obtained in both experiments, suggesting that differential retinal damage sites used in these two different experiments were sufficiently selective to partially separate foveal and parafoveal long wavelength cone systems. These observations suggest a contributory role for neural disinhibitory retinal receptor effects to explain the post-exposure spectral sensitivity functions measured in the present experiment.

The presence of retinal fibrosis complicates the explanation of the origin of the post-exposure spectral sensitivity, as alteration in normal receptor movement and orientation may be significantly altered by such fibrosis. Intracellular retinal scar formation may retard retinal receptor movement activity and other retinal reparative processes; epiretinal scar formation may result in retinal traction that has recently been suggested as a factor in peripheral visual function loss associated with human laser accident cases (6).

In addition to such retinal damage processes, previous investigations of laser-induced foveal damage have demonstrated remarkable repair of the photoreceptor matrix and partial retinal receptor regeneration (2,9,15). The presence of "glial-like" cells in the retinal histology of Cyno38 suggests the possibility of active reparative retinal tissue processes in the midst of presumably active retinal damage processes.

These retinal damage and reparative processes may contribute directly to the spectral sensitivity function as well as modulate the output of adjacent and distal neural lateral photoreceptor activity.

Cortical representation may reflect a passive projection of central retinal dysfunction onto the striate cortex via the retinal cortical projection pathways. Although considerable emphasis has usually been placed on reorganization of retinal elements in recovery, control of complex perceptual aftereffects, such as relative and absolute visual field losses reported in human laser accident cases, may reside at the level of the primary visual cortex. Stabilization and dynamic changes in size of visual field loss are occasionally disassociated with laser retinal exposure (2) and may reflect dynamics of visual cortical compensatory mechanisms.

References

1. Zwick H, Bedell RB, Bloom KR. Spectral and visual deficits associated with laser irradiation. In: Verriest G, ed. Colour Vision Deficiencies II, Mod Prob Ophthalmol Basel: Karger, 1974;13:298-306.

2. Zwick H, Bloom KR, Beatrice ES. Permanent visual change associated with punctate foveal lesions. In: Drum B, Verriest G, eds. Colour vision Deficiencies IX, 1989;251-260.

3. Harwerth RS, Sperling HG. Prolonged color blindness induced by intense spectral light in rhesus monkeys. Science 1971;174:520-523.

4. Zwick H, Beatrice ES. Long term changes in spectral sensitivity after low-level laser (515 nm exposure. In: Verriest G, ed. Color Vision Deficiencies IV, Mod Prob Opthalmol Basel: Karger, 1978;19:319-325.

5. Zwick H. Visual functional changes associated with low-level light effects. Health Physics 1989;56:657-663.

6. Zwick H, Stuck BE, Gagliano D, Parmley VC, Lund J, Molchany J, Kearney JJ, Belkin M. Two informative cases of Q-switched laser eye injury. Presidio of San Francisco, Ca: Letterman Army Institute of Research, 1991; Institute Report No 463.

7. Tootell RBH, Switkes E, Silverman MS, Hamilton SL. Functional anatomy of macaque striate cortex. II. retinotopic organization. J Neurosci 1988;8:1531-1568.

8. Padmos P, Van Norren D. The vector voltmeter as a tool to measure electroretinogram spectral sensitivity and dark adaptation. Invest Ophthal 1971;11:105-114.

9. Zwick H, Robbins DO, Reynolds SB, Lund DJ, Schuschereba ST, Long RC, Nawim M. Effects of small spot foveal exposure on spatial vision and ERG spectral sensitivity. In: Drum B, Moreland JD, Serra A, eds. Colour Vision Deficiencies X, Doc Ophthalmol Proc Ser Dordrecht: Kluver, 1991;54:581-597.

10. Karnovsky MJ. A formaldehyde-glutaraldehyde fixative of high osmolarity for use in electron microscopy. J Cellular Biology 1965;27:137a.

11. Wong-Riley M. Changes in the visual system of monocularly sutured or enucleated cats demonstrable with cytochrom oxidase histochemistry. Brain Res 1979;171:11-28.

12. Tootell RBH, Silverman MS. Two methods for flat-mounting cortical tissue. J Neuroscience Methods 1985;15:177-190.

13. Smith VC, Pokorny J. Spectral sensitivity of color-blind observers and the cone photopigments. Vision Research 1972;12:2059-2071.

14. Huang JY, Lewis A, Rasing Th. Second harmonic generation of retinal chromophores. J Phys Chem 1988;92:1755-1758.

15. Tso MOM. Photic maculopathy in rhesus monkey. Investigative Ophthalmol 1973;12:17-34.

OFFICIAL DISTRIBUTION LIST

COMMANDER
USAMRDC
ATTN: SGRD-Z/MG Travis
ATTN: SGRD-PLC/COL Sedge
SGRD-RMS/Ms. Madigan
SGRD-OP/Mr. Adams
Fort Detrick
Fredrick, MD 21701-5012

DIRECTOR
Defence Technical
Information Center
ATTN: DTIC-DDA (2 copies)
Cameron Station
Alexandria, Va 22314

COMMANDER
US Army SMO
ATTN: SLCSM-SE/Dr. Elser
SLCSM-SE/Dr. Brand
2800 Power Mill Rd.
Adelphi, MD 20783

COMMANDER
USAMSAA
ATTN: [illegible]RXSY-CSD/[illegible]. Beavers
Aberdeen Pro[illegible]q Grounds
Mary[illegible]nd 210[illegible]

COMMANDER
A[illegible]TN: STRNC-Y[illegible]D/F. Bissett
Natick RDE Center
Na[illegible]ick, MA 01760-5020

COMMANDER
USAEHA
ATTN: HSHB-MR-LL/D. Sliney
Aberdeen Proving Grounds
Maryland 21010-5422

Dr. John Ewen
OSWR/STD/STB
PO Box 1925
Washington, DC 20013

COMMANDER
HQ, USAMMDA COL Pederson
ATTN: SGRD-UMA/MAJ Walsh
Fort Detrick
Frederick, MD 21701-5009

COMMANDER
ATTN: WRDC/MLPJ/G. Kepple
WRDC/MLPJ/B.Edmonds
WRDC/MLPJ/R.Susnick
Wright Research and Development
Center, Ohio 45433

HEADQUARTERS
Department of the Army
ATTN: DASG-TLO
Washington, DC 20310

COMMANDER
USA CACDA
ATTN: ATZL-OPS-SE/MAJ Mathews
ATZL-OPS-SE/LTC Stokes
Fort Leavenworth, Kansas 66027-5300

COMMANDER
NADC
ATTN: Code 6023/Dr. Sheehy
Warminster, PA 18974-5000

COMMANDER
NMRDC
ATTN: CODE 43
National Naval Medical Ctr
Bethesda, MD 20814

COMMANDER
USAF SAM
ATTN: RZV/Dr. Farrer
RZV/LTC Cartledge
Brooks AFB, TX 78235-5301

OFFICIAL DISTRIBUTION LIST (CON'T)

OTSG
ATTN: TSG-PSP/COL Day
5109 Leesburg Pike
Falls Church, VA 22041-3258

DIRECTOR
US Army AMMRC
ATTN: AMXMR-O/Fitzpatrick
Watertown, MA 02172-0001

COMMANDER
USA Aviation Systems Cmd
ATTN: AMCPM-ALSE/H. Lee
4300 Goodfellow Blvd
St. Louis, MO 63120-1798

DIRECTOR
Defence Intelligence Agency
ATTN: DT-5A/H. Hock
Washington, DC 20340-6053

COMMANDER
USA Aeromed Research Lab
ATTN: SGRD-UAC-D/COL Karney
SGRD-UAC-D/COL Wiley
Ft. Rucker, AL 36330-5000

DIRECTOR
EWL/RSTA
ATTN: AMSEL-EW-C/J. Allen
Ft. Monmouth, NJ 07703-5303

COMMANDANT
USA Infantry School
ATTN: ATSH-CMD-D/Ken Sines
Ft. Benning, GA 31905-5400

COMMANDER
Letterman Army Institute of Research
ATTN: SGRD-ULZ (1 copy)
SGRD-UL-IR (7 copies)
Presidio of San Francisco
California 94129-6800

DIRECTOR
DARPA
ATTN: DARPA/DSO-Dr. Durvasula
1400 Wilson Blvd
Arlington, VA 22182

COMMANDER
CNVEO
ATTN: SFAE-IEN-NV(COL Michlik)
Ft Belvoir, Va 22060

DIRECTOR
Armed Forces Medical Intelligence Center
ATTN: AFMIC-SA/MAJ Krikorian
AFMIC-SA/MAJ Holahan
Fort Detrick, MD 21701-5004

DIRECTOR
DTD Directorate
ATTN: EOGWCM-CCM
WSMR, NM 88002-5519

COMMANDER
HQ TRADOC
ATTN: ATCD-ML/J.Gray
Ft. Monroe, VA 23651-5000

DIRECTOR
USA HEL
ATTN: AMXHE-IS/D. Giordano
Aberdeen Proving Grounds
Maryland 21005-5001

PRESIDENT
USA Armor & Engr Board
ATTN: ATZK-AE
Ft. Knox, KY 40121

COMMANDER
USAMRDC
ATTN:SGRD-PLC
Fort Detrick
Frederick, MD 20701-5012

OFFICIAL DISTRIBUTION LIST (CON'T)

COMMANDANT
Academy of Health Science
ATTN:HSHA-FM(LTC Lindsay)
Fort Sam Houston , TX 78236

DEAN
School of Medicine
Uniformed Service Universtiy
of the Health Science
4301 Jones Bridge Road
Bethesda, MD 20814-4799

COMMANDER
U.S Air Force School of
Aerospace Medicine
Brooks A F B, TX 78235-5000

HQDA
Assistant Secretary of the Army for
Research, Development and Acquisition
ATTN:SARD-ZT
Pentagon, Washington, DC 20310

HQDA
Assistant Secretary of the
Army for Research,Development
Acquisition
ATTN:SARD-TM
Pentagon, Washington,D.C 20310

HQDA
Deputy Chief of Staff for Operation
and Plans
Director of Training
ATTN:DAMO-TR
Pentagon, Washington,D.C 20310

HQDA
Office of the Surgeon General
ATTN:DASG-ZA
5109 Leesburg Pike
Falls Church, VA 22041-3258

HQDA
Office of the Surgeon General
Directorate of Health Care Operations
ATTN:DASG-HCO
5109 Leesburg Pike
Falls Church, VA 22041-3258

COMMANDANT
U.S Army Chemical School
ATTN:ATZN-CM-C
Fort McClellan,AL 36205-5020

COMMANDANT
U.S Army Chemical School
ATTN:ATZN-CM-S
Fort McClellan, AL 36205-5020

COMMANDANT
U.S Army Quartermaster School
ATTN:ATZM-C
Fort Lee, VA 01433-6301

COMMANDANT
U.S Army War College
ATTN:AWC-C
Carlisle Barracks, PA 17013

COMMANDANT
Command and General Staff
College
ATTN:ATZL-SW
Fort Leavenworth,KS 66027-5000

COMMANDANT
Academy of Health Sciences,U.S Army
ATTN:AHS-COM
Fort Sam Houston, TX 78234-6100

Dean
U.S Army School of Aviation
Medicine
ATTN:HSHA-AVN
Fort Rucker, AL 36362-5377

COMMANDER
US Army Medical Research and
Development Command
ATTN:SGRD-ZC(COL Dangerfield)
Fort Detrick, Fredrick,MD 21702-5012

COMMANDER
USAMRDC
ATTN:SGRD-ZS(COL Schakenburg)
Fort Detrick, Frederick, MD 21702-5012